# A Persistent Surface Inversion Event in Armenia as Simulated by WRF Model


Artur Gevorgyan[1]
e-mail: agm86@yandex.ru

Hamlet Melkonyan[1]
e-mail: hamlet_melkonyan@yahoo.com

Rita Abrahamyan[1]
e-mail: rita_60@mail.ru

Zarmandukht Petrosyan[1]
e-mail: edittaron@gmail.com

Anna Shahnazaryan[2]
e-mail: shz.ann91@gmail.com

Hrachya Astsatryan[2]
e-mail: hrach@sci.am

Vladimir Sahakyan[2]
e-mail: svlad@sci.am

Yuri Shoukourian[2]
e-mail: shouk@sci.am

1- Armenian State Hydrometeorological and Monitoring Service (Armstatehydromet), Yerevan, Armenia
2- Institute for Informatics and Automation Problems; Yerevan, Armenia



## ABSTRACT

The case study on strong temperature inversion event in Armenia has been presented in this paper using observed temperatures and simulations from both global (ERA-Interim) and regional high-resolution (WRF) models. According to the observations the December of 2013 was ranked as the second coldest since 1961. Monthly mean temperature anomaly for entire Armenia consisted of -4.4 ˚C in December, while that for inversion affected basins such as Ararat valley was -9 -7 ˚C. The persistent temperature inversion in Ararat valley lasted more than two weeks resulted in unprecedented cold wave events. The ability of the global ERA-Interim and regional WRF models to simulate this dramatic temperature event in Armenia has been examined. The results show that high resolution WRF model has a clear advantage over ERA-Interim model in representation of spatial temperature pattern in Armenia. The small-scale variations of temperature and surface inversion basins are simulated by WRF model while ERA-Interim model provides very coarse results underestimating the spatial variability and influence of topography. However, it should be noted that there are significant uncertainties and errors in WRF temperature forecasts. Significant RMSE values and negative correlation coefficients obtained for the area covering inversion basin indicate that WRF model fails to capture the temporal variability of temperature during the inversion event. It is worth noting the significant positive bias for daytime WRF temperatures during the strongest phase of the inversion.



## Keywords

WRF model; temperature inversion; Ararat Valley; topography


## 1. INTRODUCTION

Armenia and South Caucasus region are characterized by complex geography and large-scale atmospheric circulations. The region contains several large water bodies and significant topography, including Caucasus mountains in the north and north-east, mountain ranges and plateaus of the Armenian Highland stretching from west to east and the Kura-Araks plain located in the east. The orography of the study region has a special influence on the weather systems coming from the outside and passing over it producing its own systems with certain properties peculiar to the plateau. The atmospheric circulation in winter season is highly variable in Armenia. During winter, Armenia may be influenced by polar, and arctic (rarely) air masses which can be of both continental and maritime origins modified by continental influence. Intrusion of cold air masses from the north and maintenance of anticyclonic circulation are favorable conditions for formation strong surface inversions in closed basins and valley regions of Armenia such as Ararat Valley, Shirak plateau, etc. These synoptic-scale systems and the influence of topography make the winter circulation and the spatial distribution of precipitation, temperature and wind quite complicated in this region.

The strong and persistent inversion was observed in Armenia in December 2013 causing low temperatures in inversion affected regions. The aim of this article is to examine surface inversion in Armenia using observations and simulations from high resolution regional model and global model output data. Section 2 presents the description of the observed data and models output data used in this study. Description of main results is presented in Section 3. Conclusions and discussions are presented in Section 4.

## 2. DATA AND METHOD

The experiments cover the winter period of 2013 based on the series of daily simulations with the WRF (Weather Research and Forecast) model (Michalakes et al 1998; Michalakes et al 2004), which is a non-hydrostatic next-generation mesoscale forecast model and widely used by many institutes and meteorological services around the world. WRF allows the selection among a large number of parameterization schemes of various physical processes. WRF model outputs are used in operational forecasting of the short-term forecasts. WRF model is initialized using NCEP Global Forecast System analysis and forecasts at 0.5 deg horizontal resolution (Whitaker et al. 2008). Data produced during pre-processing and simulations of WRF are in the Lambert conformal projection, which is well-suited for mid-latitude domains. The weather forecasts are performed on a daily basis, using the following 1-way nesting strategy. The parent domain D1 covers the major part of Europe and the all Caucasus and some parts of the Central Asia and the Middle East (40.0_ N, 44.7_ E) with 202×202 grid points at a 18-km resolution, the nest domain D2 (3-km horizontal grid increment) covers the whole territory of Armenia with

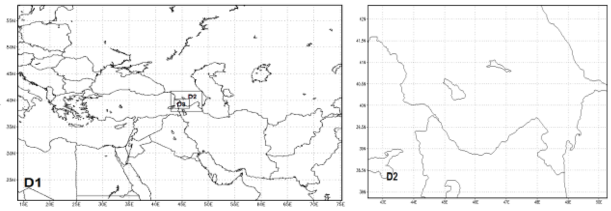


202×202 grid points Fig. 1.

a b

Figure 1. WRF domains: coarse domain D1 (a) and nested domain D2 (b)

The model uses vertical 31 eta_levels, and the geographic data resolution is 30 seconds. The model was initialized with the initial and boundary conditions of Global Forecast System (GFS) at 00:00 UTC (local time on 04:00) for 10-day period, namely 14-16 December 2013 and 28 December 2013 to 03 January 2014.

Based on preliminary investigations (Hovsepyan et al. 2013), the following parameterizations have been implemented in the present study:

The model physics package includes the WRF Single Moment 6-class scheme for cloud microphysics with ice, snow and graupel processes suitable for high-resolution simulations (Hong and Lim 2006)

The Kain-Fritsch scheme with deep and shallow convection sub-grid parameterization using mass flux approach with downdrafts and CAPE removal time scale (Kain 1993).

The planetary boundary layer was given by the Yonsei University scheme (YSU PBL) with non-local explicit entrainment layer and parabolic profile in unstable mixed layer (Michalakes et al 1998; Michalakes et al 2004)

The NOAA land surface model (Unified NCEP/NCAR/AFWA scheme with soil temperature and moisture in four layers, fractional snow cover and frozen soil physics ) was used for the land surface, the rapid radiative transfer model (RRTM) longwave scheme used for longwave radiation, and the Dudhia shortwave scheme used for the atmospheric radiation processes.

High performance computing resources (up to 512 cores) of Armenian national grid infrastructure (Armenian National Grid Intitiative, http://www.grid.am) have been used for conducting the series of experiments.

To compare results from high-resolution WRF regional model with those from general circulation model (GCM) forecasted values of 6-hourly surface temperatures from the European Centre for Medium-Range Weather Forecasts (ECMWF) ERA-Interim model with lag of 03 and 12 h were also considered in this paper (Dee et al. 2011; Berrisford et al. 2011). The ERA-Interim atmospheric model and reanalysis system uses cycle 31r2 of ECMWF's Integrated Forecast System (IFS), which was introduced operationally in September 2006. Forecast data on pressure levels and for the surface and single level parameters are archived at the 28 ranges, or steps from daily forecasts at 00:00 and 12:00 UTC. On the ECMWF Data Server forecasts are only available for surface and single level fields and only up to a range of 12 h. The dataset has a horizontal resolution of T255 (on a 0.75° . 0.75° grid). The ability of ERA-Interim data to represent regional-scale and large-scale circulations over Armenia and South Caucasus region has been considered previously (Gevorgyan 2012; Gevorgyan 2013; Gevorgyan and Melkonyan 2014; Gevorgyan 2014). Overall, it was shown that the ERA-Interim data captures key features of the regional and large-scale circulation.

Observed 2-metre temperatures from all current 47 operational stations in Armenia (Vardanyan et al., 2013) are used to study surface inversion in Armenia in December 2013, and to compare output from WRF model with observations. The observed 3-hourly temperature data sets were taken from Armenian State Hydrometeorological and Monitoring Service (Armstatehydromet). Prior to the analysis, basic quality control on observed temperatures data derived from stations was applied.

There are different statistical measures for verification of the performance of models quantitatively (Evans et al ., 2004; Wilks, 2006; Gevorgyan 2012). In this paper, 2-metre temperature forecasts from the WRF model are evaluated against observations using the statistics presented below.

The root-mean-square error (RMSE) was used to assess the errors of temperature forecasts from WRF model making use of Equation (1).

$$RMSE = \sqrt{\frac{\sum_{i=1}^{n}\left(O(i)-F(i)\right)^2}{n}} \qquad (1)$$

where O(i) – observed temperature in i-th day of the verification period, F(i) – forecasted temperature in i-th day of the verification period n – total number of days included in the verification period.

To test the ability of WRF model to capture the temporal variability of the observed temperature in Armenia the correlation coefficient (R) between the forecasts and observations of temperature was calculated making use of Equation (2).

$$R = \frac{\sum_{i=1}^{n}(O(i)-\overline{O})(F(i)-\overline{F})}{\sqrt{\sum_{i=1}^{n}(O(i)-\overline{O})^2\sum_{i=1}^{n}(F(i)-\overline{F})^2}} \qquad (2)$$

where again, O(i) – observed temperature in i-th day of the verification period, F(i) – forecasted temperature in i-th day of the verification period, while –observed mean temperature, – forecasted mean temperature, and n – total number of days included in the verification period.

The spatial variability of temperature obtained from observed and forecasted data was estimated through standard deviation of temperature, showing the range of temperature around the mean values (Equation 3)

$$\sigma = \sqrt{\frac{\sum_{i=1}^{n}\left(T(i)-\overline{T}\right)^2}{(n-1)}} \qquad (3)$$

where – standard deviation, since we used to study spatial variability of observed and forecasted temperatures here T(i) – observed/forecasted temperatures in i-th station, – observed/forecasted spatial mean temperatures, n – total number of stations included in the verification.

# 3. RESULTS

## 3.1. Characteristics of the basin inversion and its evolution simulated by WRF data and by Observations

In order to study the spatial pattern of basin inversion we examined the distribution of mean temperatures in Armenia using observations and models output data. The period from 29th December to 31th December of 2013 covering the most intense phase of surface inversion has been selected during which very low temperatures were observed in Yerevan and over low-elevated parts of Ararat Valley. The surface temperature inversion can be clearly seen in Figure 2a showing the distribution of mean early morning observed temperatures from all 47 meteorological stations of Armenia. Ararat Valley in the south-west of Armenia including Yerevan, Shirak Marz in north-west of Armenia and several valley stations in the south-west of Armenia are strongly influenced by temperature inversion. Accumulation of cold air in the mentioned regions caused low observed temperatures lower than -16 $^0$C. It is worth noting that mean temperature at high mountain station Aragats (at 3229 m above sea-level) was significantly higher (varying from -10 to -8 $^0$C) relative to the temperatures observed in the inversion basin. The inversion-free regions in the northeastern (Tavush marz) and southeastern (Syunik marz) regions are also characterized by relatively high temperatures varying mainly from -6 to 0 $^0$C (Figure 2a). It can be seen from Figure 2b that WRF model overestimates temperatures relative to observations over the inversion basin showing warmer temperatures varying mainly from -16 to -14 $^0$C. However, it is worth noting the cold area over northwest of Armenia (Shirak marz) simulated by WRF model with average temperatures lower that -16 $^0$C. This region was the coldest during the inversion event with the lowest observed temperatures varying from -28 to -22 $^{0}$C. WRF model also successfully simulates relatively high temperatures over highly elevated parts of Aragats mountain and over inversion-free northeastern and southeastern regions of Armenia (Figure 2b). By contrast ERA-Interim model provides very general and smooth picture of spatial distribution of temperature over Armenia (Figure 2c). ERA-Interim simulated mean temperatures vary within very narrow range from -16 to -12 $^{0}$C over entire Armenia. ERA-Interim model fails to reproduce spatial variations of temperature in Armenia associated with influence of topography. This is due to coarse spatial resolution of ERA-Interim model (80 km).

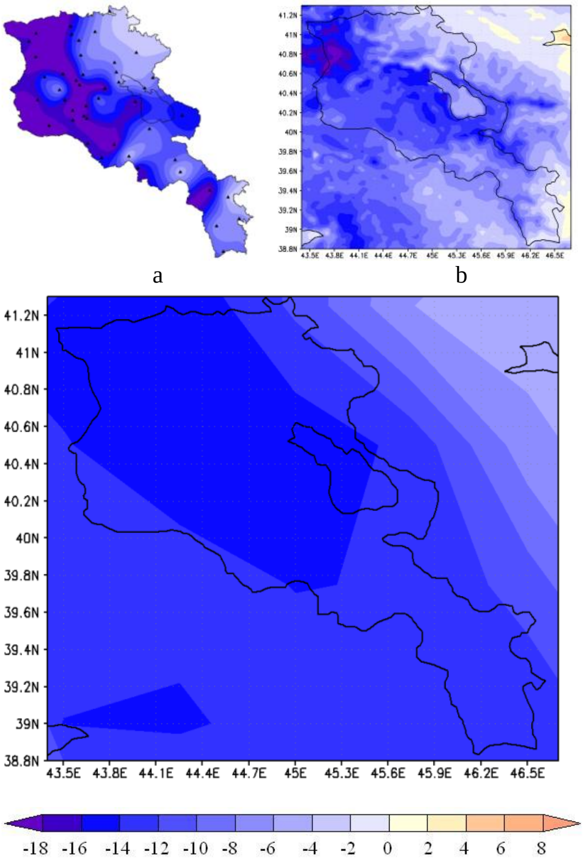


Figure 2. Mean observed (a) and 3-hour forecasted surface temperatures ($^{0}$C) from WRF (b) and ERA-Interim (c) models at 0300 UTC for the period 29-31 December of 2013

The spatial pattern of the observed daytime (at 1200 UTC or at 1600 local time) temperatures over Armenia for 29-31 December shows that surface inversion is significantly enhanced (Figure 3a). Surface inversion and cold air maintain over closed plateaus of northwest and Ararat valley leading to very low temperatures not exceeding -13 $^{0}$C. These low temperatures are partly due to low-level clouds significantly limiting surface heating from sun during day. On the other hand, temperatures in the northeastern and southeastern regions are as high as 4-6 $^{0}$C. Figure 3 b shows that the main tendency of temperature change showing increase of daytime temperature from south-west (Ararat Valley) and north-west (Shirak marz) to north-east and south-east is captured successfully by WRF model. However, temperatures over inversion basins including Ararat valley and Shirak marz are strongly overestimated by WRF model showing significantly warmer temperatures (from -8 to -4 °C) relative to observations (from -15 to -12 °C). Mean temperatures from WRF model are positive over warm northeastern and southeastern regions of Armenia and consist of 0-4 $^{0}$C. It is worth noting that ERA-Interim 12-hour forecasts of temperatures fail to reproduce both the temperature pattern and mean values of daytime temperatures over entire Armenia (Figure 3c). ERA-Interim simulated mean temperatures vary within very narrow range from -16 to -12 $^{0}$C over entire Armenia.

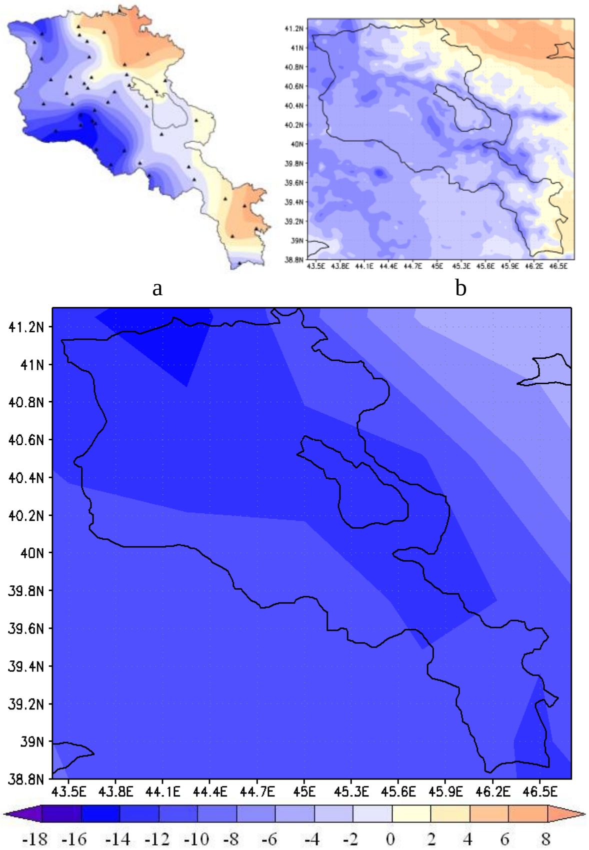


Figure 3. Mean observed (a) and 12-hour forecasted surface temperatures ($^{0}$C) from WRF (b) and ERA-Interim (c) models at 1200 UTC for the period 29-31 December of 2013

Figure 4a shows that the spatial pattern of mean observed temperature for 29-31 December at 0000 UTC in Armenia is very similar to that at 0300 UTC (Figure 2a). However, WRF-simulated mean temperature pattern at 0000 UTC obtained from 24-hour forecasts (Figure 4b) differs from the WRF mean temperature pattern at 0003 UTC obtained from 3-hour forecasts presented in Figure 2b. The spatial variability for 24-hour temperature forecasts is significantly reduced relative to that of 3-hour forecast. Firstly, the 24-hour forecasted temperatures over northwestern Shirak marz are higher (from -16 to -14 $^{0}$C) than 3-hour temperature forecasts leading to greater positive bias relative to observations for this region. Second, the warm area over mountain Aragats disappeared in 24-hour forecasts in contrast to observations (Figures 4a-b).

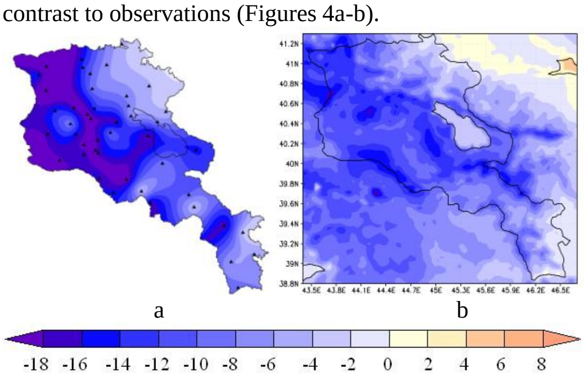


Figure 4. Mean observed (a) and 24-hour forecasted surface temperatures ($^{0}$C) from WRF model (b) at 0000 UTC for the period 29-31 December of 2013

On the other hand, 24-hour temperature forecast clearly indicates inversion basin area over low-elevated parts of Ararat valley (in the south-west) indicating stronger influence of topography on temperature distribution. However, again, forecasted temperatures are warmer than observations.

In this Section we examine the ability of WRF model to simulate temporal variability of temperature over Ararat valley during the persistent temperature event. For that reason four stations located in lower parts of Ararat Valley have been selected (Table 1). After that, the closest grid-points to each of the station have been used from WRF grid. It is worth noting that both distance and altitude differences between stations and the selected WRF grid-points have been considered. 2 metre temperature data from the stations and selected grid-points are further considered for verification of temperature forecasts over Ararat basin. We focused on the beginning of the inversion event started on 14-15th December, the strongest phase of inversion (end of December) and the end of the event (beginning of the January of 2014).

Table 1. Selected stations from Ararat Valley for verification of WRF temperature forecasts. Distance and altitude differences between stations and selected WRF grid-points (in meters) are indicated with ΔD and ΔH, respectively

| N | Station | Height above sea-level, m | ΔD, m | ΔH, m |
|---|---|---|---|---|
| 1 | Armavir | 870 | 2,000 | 5,0 |
| 2 | Artashat | 829 | 2,000 | 0,0 |
| 3 | Ararat | 818 | 2,000 | 0,0 |
| 4 | Merdzavan | 942 | 1,500 | 4,0 |

Time series of mean observed and predicted temperatures over Ararat Valley for the beginning, the strongest phase and the end of the inversion event are presented in Figures 5 a-c. Generally, WRF model underestimates mean temperatures over Ararat Valley in the beginning of the inversion event (14-16 December) resulting in the negative biases between WRF simulated temperatures and observations for all forecast ranges, i.e. 3-hour, 12-hour and 24-hour forecasts. However, WRF model agrees with observation showing temperature decrease from 14th to 15th December (Figures 5a-b). By contrast, WRF model simulate significantly warmer temperatures for the strongest phase of the inversion (28-31 December), the positive bias for daytime (1200 UTC) temperatures is as high as 8 $^0$C on average (Figure 5 b). WRF model fails to capture temperature tendency for the end of temperature inversion event. Temperature changes from observations and WRF model are of opposite sign from 1th to 4th of January resulting in strong negative bias between WRF temperature forecasts and observations (-10 $^0$C for 24-hour forecasts (Figure 5 c) from 2th to 4th January). Overall, the results show that WRF model does not reproduce temporal variability of temperature accurately over Ararat basin. It is interesting to note, that both observed and modeled data show the lowest spatial variability obtained for daytime temperatures since the 28th December (Figure 5 b, doted lines).

Mean estimates of verification of WRF temperature forecasts over low-elevetad parts of Ararat Valley for the entire 10-days period are presented in Table 2. The lowest temperature bias (in terms of absolute value) was obtained for very short range 3-hour forecasts (0,6 $^0$C), while the bias for 12-hour forecasts consists of 2,3 $^0$C and that for 24-hour forecasts consists of -2,4 $^0$C. Significant RMSE values (from 6,1 to 6,2 0C) and negative correlation coefficients (from -0,20 to -0,12) indicate that WRF model fails to capture the temporal variability of temperature during the inversion event over Ararat basin as it can be seen from Figures 5a-c.

Table 2. Mean estimates of verification of temperature forecasts over low-elevetad parts of Ararat Valley (less than 1000 m above sea-level) for the entire 10-days period (ME - temperature bias, RMSE - root-mean-square error and R – correlation coefficient)

| Lag, h | ME, $^0$C | RMSE, $^0$C | R |
|---|---|---|---|
| 3 | 0,6 | 6,1 | -0,20 |
| 12 | 2,3 | 6,1 | -0,26 |
| 24 | -2,4 | 6,2 | -0,12 |

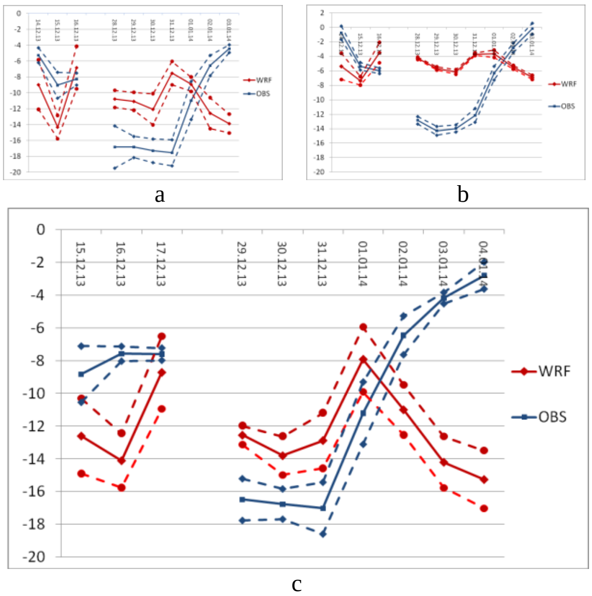


Figure 5. Time-series of observed (blue lines) and forecasted surface temperatures (0C) from WRF model (red lines) averaged over low-elevetad parts of Ararat Valley (less than 1000 m above sea-level) for the entire 10-days period (from December, 2013 to January, 2014). Dotted lines indicate standard deviations around mean values (±σ) . a) 3-hour forecasts at 0300 UTC; b) 12-hour forecast at 1200 UTC; c) 24-hour forecasts at 0000 UTC

# 4. CONCLUSIONS

The case study on strong temperature inversion event in Armenia has been presented in this paper using observed temperatures and simulations from both global (ERA-Interim) and regional high-resolution (WRF) models. According to the observations the December of 2013 was ranked as the second coldest since the 1961. Monthly mean temperature anomaly for the entire Armenia consisted of -4.4 $^0$C in December, while that for inversion affected basins such as Ararat valley was -9 -7 $^0$C. The persistent temperature inversion in Ararat valley lasted more than two weeks resulted in unprecedented cold wave events. Mean daily temperatures in Yerevan were lower than norm by more than 6 $^0$C since the middle of December, and in the end of December the negative temperature anomaly consisted of -14 to -13 $^0$C.

The ability of the global ERA-Interim and regional WRF models to simulate this dramatic temperature event in Armenia has been examined. The results show that high resolution WRF model has a clear advantage over ERA-Interim model in representation of spatial temperature pattern in Armenia associated with topography influence. The small-scale variations of temperature and surface inversion basins are simulated by WRF model while ERA-Interim model provides very coarse results underestimating the spatial variability and influence of topography. The latter is expected, since the General Circulation Models can simulate the large-scale mean climate conditions and its evolution to a great extent, while their ability to simulate climate features at a regional scale is limited. However, it should be noted that there are significant uncertainties and errors in WRF temperature forecasts as can be seen from the verification results. Significant RMSE values and negative correlation coefficients obtained for the area covering inversion basin indicate that WRF model fails to capture the temporal variability of temperature during the inversion event. It is worth noting the significant positive bias for daytime WRF temperatures during the strongest phase of the inversion (28-31 December) reaching up to 8 $^{0}$C on average for 12-hour range forecasts.

Despite the high resolution of WRF model (3 km), an even finer grid is necessary to resolve the detailed topography and to correctly simulate local processes such as surface temperature events. An accurate modeling of the planetary boundary layer (PBL) over finescale orography is particularly important for the studied process. Future work should test the model sensitivity to various parameterizations such as the PBL physics and verification of other surface meteorological elements (pressure, wind, humidity) and vertical profiles of temperature, wind and humidity during this dramatic inversion event in Armenia.

## 5. ACKNOWLEDGEMENTS

The work has been done within the framework of the state target programme entitled “Applying of a National Research e-Infrastructure for Solving the Natural Sciences' Problems” together with the specialists of the Institute for Informatics and Automation Problems of the National Academy of Sciences of the Republic of Armenia and Armenian State Hydrometeorological and Monitoring Service.

## REFERENCES

[1] Armenian National Grid Intitiative, http://www.grid.am.

[2] Berrisford P., Dee D., Poli P., Brugge R., Fielding K., Fuentes M., Kallberg P., Kobayashi S., Uppala S., Simmons A. (2011) The ERA-Interim archive: Version 2.0. ERA Report Series 1:23.

[3] Dee D., Uppala S.M., Simmons A.J., Berrisford P., Poli P., Kobayashi S., Andrae U., Balmaseda M.A., Balsamo G., Bauer P., Bechtold P., Beljaars A.C.M., van de Berg L., Bidlot J., Bormann N., Delsol C., Dragani R., Fuentes M., Geer A.J., Haimberger L., Healy S.B., Hersbach H., H´aolm E.V., Isaksen L., Kallberg P., Kohler M., Matricardi M., McNally A.P., Monge-Sanz B.M., Morcrette J.J., Park B.K., Peubey C., de Rosnay P., Tavolato C., Thepaut J.N., Vitart F. (2011) The ERAinterim reanalysis: configuration and performance of the data assimilation system. Q J R Meteorol Soc 137:553–597.

[4] Evans J.P., Smith R.B., Oglesby R.J. (2004) Middle East climate simulation and dominant precipitation processes. Int J Climatol 24:1671–1694.

[5] Gevorgyan A. and Melkonyan H. (2014) Regional impact of the Armenian Highland as an elevated heat source: ERA-Interim reanalysis and observations. Climate Dynamics 44:1541–1565. DOI: 10.1007/s00382-014-2236-z

[6] Gevorgyan A. (2014) Surface and tropospheric temperature trends in Armenia. Int J Climatol 34: 3559–3573. doi:10.1002/joc.3928

[7] Gevorgyan A. (2013) Main types of synoptic processes and circulation types generating heavy precipitation events in Armenia. Meteorol Atmos Phys 122:91–102.

[8] Gevorgyan A. (2012) Verification of daily precipitation amount forecasts in Armenia by ERA-Interim model. Int J Climatol 33(12):2706–2712.

[9] Gevorkian R.G., Aslanian A.T., Armenia, Encyclopedia of Earth Science, Encyclopedia of European and Asian Regional Geology, ISBN: 978-0-412-74040-4 1997, pp 26-34.

[10] Hong Song-You, Lim Jeong-Ock J., The WRF Single-Moment 6-Class Microphysics Scheme (WSM6), J. Korean Meteor. Soc., Vol. 42, No. 2. (2006), pp. 129-151.

[11] Hovsepyan A., Petrosyan Z., Abrahamyan R., Melkonyan H., Shahnazaryan A., Astsatryan H., Khotsanyan T., Sahakyan V., Shoukourian Yu., Prediction of hydrometeorological hazardous events in Armenia by implementing WRF-ARW physics sensitivity experiments: a case study for heavy rainfall, Proceedings of the International Conference on Computer Science and Information Technologies (CSIT'2013), pp. 403-406, Yerevan, Armenia, September 23-27, 2013.

[12] Kain J.S., Fritsch J.M., Convective parameterization for mesoscale models: The Kain–Fritsch scheme. The Representation of Cumulus Convection in Numerical Models, Meteor. Monogr., No. 24, Amer. Meteor. Soc., 165–170, 1993.

[13] Michalakes, J., Dudhia J., Gill D., Henderson T., Klemp J., Skamarock W., and Wang W., 2004: The Weather Research and Forecast Model: Software Architecture and Performance, Proceeding of the Eleventh ECMWF Workshop on the Use of High Performance Computing in Meteorology, 25–29 October 2004, Reading, U.K.

[14] Michalakes J., Dudhia J., Gill D., Klemp J. and SkamarockW. Design of a next-generation regional weather research and forecast model: Towards Teracomputing, World Scientific, River Edge, New Jersey, 1998, pp. 117-124.

[15] Second National Communication Report, Ministry of Nature Protection of the Republic of Armenia, 2010, p.132

[16] Vardanyan L., Melkonyan H., Hovsepyan A. (eds). 2013. Current status and Perspectives for Development of Climate Services in Armenia. Ministry of Emergency Situations of Republic of Armenia: Yerevan, 40.

[17] Whitaker Jeffrey S., Thomas M. Hamill, Xue Wei, Yucheng Song, ZoltanToth, 2008: Ensemble Data Assimilation with the NCEP Global Forecast System. Mon. Wea. Rev., 136, pp. 463–482., 2008, doi: http://dx.doi.org/10.1175/2007MWR2018.1.

[18] Wilks D.S., Statistical methods in the atmospheric sciences. Elsevier, Burlington, 2006 .